ELSEVIER

Biophysical Chemistry 106 (2003) 179–192

Biophysical Chemistry

www.elsevier.com/locate/bpc

Temperature dependency and temperature compensation in a model of yeast glycolytic oscillations

Peter Ruoff[a,*], Melinda K. Christensen[a], Jana Wolf[b], Reinhart Heinrich[b]

[a]*School of Science and Technology, Stavanger University College, P.O. Box 8002, Ullandhaug, N-4068 Stavanger, Norway*
[b]*Institute of Biology, Humboldt-University Berlin, Invalidenstrasse 42, D-10115 Berlin, Germany*

Received 17 February 2003; received in revised form 30 June 2003; accepted 1 July 2003

Abstract

Temperature sensitivities and conditions for temperature compensation have been investigated in a model for yeast glycolytic oscillations. The model can quantitatively simulate the experimental observation that the period length of glycolytic oscillations decreases with increasing temperature. Temperature compensation is studied by using control coefficients describing the effect of rate constants on oscillatory frequencies. Temperature compensation of the oscillatory period is observed when the positive contributions to the sum of products between control coefficients and activation energies balance the corresponding sum of the negative contributions. The calculations suggest that by changing the activation energies for one or several of the processes, i.e. by mutations, it could be possible to obtain temperature compensation in the yeast glycolytic oscillator.

Keywords: Temperature compensation; Glycolysis; Biochemical oscillations; *Saccharomyces cereviciae*; Mathematical modelling; Metabolic control theory; Cellular systems

1. Introduction

Many biological oscillators have important regulatory functions of physiological processes and in the adaptation of organisms to their environments. Circadian rhythms, for example, have clock or timing functions [1–4]. Because of this, periods in these biological clocks are compensated against environmental influences such as temperature, pH and nutritional conditions. Among the environmental compensation mechanisms, temperature compensation in circadian clocks is one of the best documented [1,2,5,6]. Temperature compensation means that within a physiological temperature range the rhythm's period length remains nearly constant at different (but constant) temperatures, despite the fact that most of the underlying individual (enzyme-catalyzed) processes are quite dependent on temperature. In general, the Q_{10} of enzyme-catalyzed processes lies in the range of 2 [7], which means that the reaction rate doubles as the temperature increases by 10 °C.

Although the existence of temperature compensation of biological clocks is well documented, little is known about how these compensation

*Corresponding author. Tel.: +47-51-831887; fax: +47-51-831750.
E-mail address: peter.ruoff@tn.his.no (P. Ruoff).

0301-4622/03/$ - see front matter © 2003 Elsevier B.V. All rights reserved.
doi:10.1016/S0301-4622(03)00191-1

mechanisms operate. Hastings and Sweeney [8] were the first to suggest the existence of opposing reactions controlling the period of biological clocks similar to the opposing processes occurring in a temperature-compensated mechanical pendulum or in modern temperature-compensated electronic clocks [9]. A theory of opposing reactions [10,11] can be formulated on the basis of positive and negative elements that are apparently present in any reaction kinetic oscillator. A brief description of this theory will be given below. Other proposals concerning the origin of temperature compensation have focused on the importance of diffusion-controlled processes or opposing processes within enzyme catalysis (for a review see Ref. [9]).

While temperature compensation is advantageous for the action of biological clocks, there are only few examples of temperature-compensated processes within pure chemical or biochemical oscillators. Skrabal [12] was probably the first to report a temperature-overcompensated process, i.e. a process where the overall reaction rate decreases as temperature increases. Besides the early work by Skrabal we are aware of only two other reports [13,14] which experimentally described and modelled temperature compensation of a chemical oscillator.

Biochemical oscillations, such as the oscillatory glycolysis [15–19] are important experimental systems for understanding the dynamics and regulation of biological rhythms. However, chemical as well as biochemical oscillators are generally not temperature-compensated. Because temperature compensation is an important aspect in many biological clock rhythms, we wondered whether it would be possible, at least in theory, to construct a temperature-compensated biochemical oscillator. As a target system we chose the glycolytic oscillator in yeast cells, because the oscillations are easily generated, and intensively studied. Moreover, a wide spectrum of yeast mutants is available. In this work we investigated how temperature compensation can occur in a model of glycolytic oscillations in yeast cells developed by some of us [20]. Our results show that a 'balance' in activation energies of opposing processes appears necessary to observe temperature compensation. Similar observations have also been made in a theoretical temperature-sensitivity study of the *Drosophila* circadian oscillator [21,22] and the oscillatory peroxidase–oxidase reaction [23].

Our theoretical analysis is based on data on the temperature dependency of glycolytic oscillations in suspensions of yeast cells by Betz and Chance [24] and by unpublished work of Hemker, Bakker, Teusink, Richard, Westerhoff and van Dam. These data demonstrate that the frequency of the oscillations increase with temperature between 5 and 40 °C. A corresponding increase in frequency with increasing temperature has also been observed in yeast cell extracts by Z. Yuan, K. Tsuji and S.C. Müller (unpublished).

2. Condition for temperature compensation in reaction kinetic oscillators

Temperature compensation means that the oscillator's period is nearly constant at different temperatures as long as the temperature is held constant during the oscillations. Experimentally, temperature compensation is normally observed only in a certain—for the organism physiologically important—temperature interval, while outside of this interval the period may rapidly change or oscillations may no longer be observable. Also in a recently discovered chemical temperature-compensated oscillator [13,14] temperature compensation occurs only in a limited temperature interval.

The type of mathematical model we consider here consists of a set of coupled differential equations describing how the metabolite concentrations S_i change in time

$$\frac{\mathrm{d}S_i}{\mathrm{d}t} = \sum_i n_{ij} v_j \tag{1}$$

In these equations, the parameters n_{ij} denote stoichiometric coefficients of the reaction system and v_j are the reaction rates of the individual processes [25,26]. The reaction rates are functions of the rate constants and the metabolite concentrations. A reasonable assumption to make is that the temperature dependence of the rate constants k_j is described by the Arrhenius-equation

$$k_j = A_j \mathrm{e}^{E_j/RT} \tag{2}$$

where A_j is a pre-exponential factor, E_j is the activation energy of process j, T is the temperature in Kelvin and R is the gas constant. The A_j's and E_j's may be considered as temperature-independent constants. In the case where rapid-equilibrium constants K_l are included in the rate equations, the temperature-dependence of K_l can be described in an analogous way as by Eq. (2), i.e. by substituting the activation energy with the enthalpy ΔH_l^0. In this case the pre-exponential factor can still be treated as temperature-independent and becomes $A_l = \exp(-\Delta S_l^0/R)$ [27].

The temperature dependence of the oscillator's period P will be a function f of the rate and equilibrium constants, i.e.

$$P = f(k_j(T),\ K_l(T)) \tag{3}$$

To find the condition for temperature compensation in a temperature interval around a certain reference temperature $T = T_{\mathrm{ref}}$, we start from $\mathrm{d}P/\mathrm{d}T$ at this point

$$\frac{\mathrm{d}P}{\mathrm{d}T} = \sum_j \frac{\partial f}{\partial k_j}\frac{\mathrm{d}k_j}{\mathrm{d}T} + \sum_l \frac{\partial f}{\partial K_l}\frac{\mathrm{d}K_l}{\mathrm{d}T} \tag{4}$$

Using Eq. (2) for calculating the derivatives $\mathrm{d}k_j/\mathrm{d}T$ and inserting the resulting expression (and analogous expression for $\mathrm{d}K_l/\mathrm{d}T$) into Eq. (4) yields

$$RT^2\frac{\mathrm{dln}\,P}{\mathrm{d}T} = \sum_j \frac{\partial \ln f}{\partial \ln k_j}E_j + \sum_l \frac{\partial \ln f}{\partial \ln K_l}\Delta H_l^0 \tag{5}$$

The terms $\partial \ln f/\partial \ln k_j$ and $\partial \ln f/\partial \ln K_l$ can be considered as sensitivity coefficients which in the context of metabolic regulation are called 'control coefficients' C_j and C_l, respectively [25,28,29].

Temperature compensation of the oscillations requires $\mathrm{dln}\,P/\mathrm{d}T = 0$. In general, the C_j's depend on the kinetic constants k_j, such that the condition for temperature compensation from Eq. (5) becomes only approximately valid within a certain temperature range. For such a local temperature range the condition for temperature compensation can be formulated as

$$\sum_i C_i E_i \cong 0 \tag{6}$$

where index 'i' runs over all rate constants and (rapid) equilibrium constants (if present in the system). In reaction kinetic oscillators there are often distinct positive and negative contributions to the period, which are reflected by positive or negative C_i values [10]. These positive and negative contributions appear to be necessary (but not sufficient) elements for physico-chemical oscillations to occur. The simultaneous occurrence of positive and negative feedbacks, which appear to be present in all physico-chemical oscillators has been described by Franck [30] as 'antagonistic feedback'.

An alternative way to formulate the condition of temperature compensation, Eq. (6), is to separate both negative and positive contributions. This leads to an 'antagonistic balance equation' with the 'opposing' positive (α) and negative (β) contributions on each side of the equation

$$\sum_\alpha C_\alpha E_\alpha \cong -\sum_\beta C_\beta E_\beta \tag{7}$$

Eq. (7) can be considered as a generalization of the proposal by Hastings and Sweeney [8] where opposing reactions are already contained within any oscillator model [10] and need not necessarily lie outside of the oscillator's reaction network.

3. The model

The mechanism of the oscillatory glycolysis was found to be strongly dependent on the kinetic properties of the key enzyme phosphofructokinase (PFK) [31]. PFK is activated by its substrate, fructose 6-phosphate, by its product, ADP and, in some cases, by its second product, fructose 1,6-bisphosphate. ATP acts at higher concentrations as an inhibitor, whereas AMP activates PFK. Although models which describe glycolytic oscillations vary in complexity [32–37], they are mostly based on one or several of the regulatory properties of PFK. The model we consider here is based on the cooperative inhibition of PFK by ATP and was previously used to study the effect

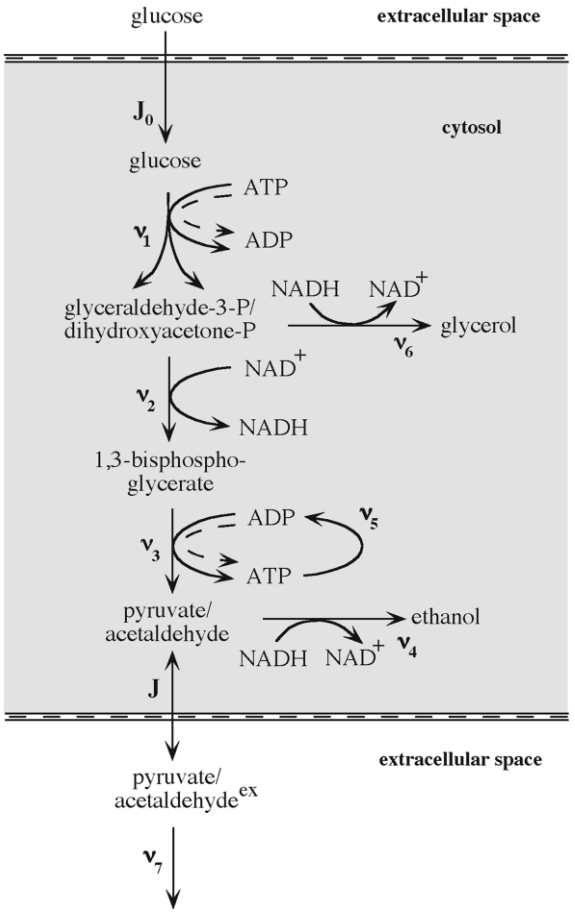

Fig. 1. Reaction scheme for the glycolytic model [20] showing the main reactions of anaerobic glycolysis in a yeast cell together with the influx and outflux of glucose and pyruvate/acetaldehyde, respectively.

of intercellular coupling on the synchronization of individual oscillating yeast cells [20]. Here we assume that all cells are synchronized and consider, therefore, the reactions in only one single cell. The reaction network leading to oscillatory glycolysis in a single cell is shown in Fig. 1 and represent the following: J_0 is the input flux of glucose through the cellular membrane; v_1 is the reaction velocity of the combined reactions of hexokinase, phosphoglucoisomerase and PFK; v_2 is the velocity of the glyceraldehyde-3-phosphate dehydrogenase reaction; v_3 is the velocity of the combined reactions of phosphoglycerate kinase, phosphoglycerate mutase, enolase and pyruvate kinase; v_4 is the velocity of the alcohol dehydrogenase reaction; v_5 is the velocity of nonglycolytic ATP-consumption; v_6 is the velocity for forming glycerol from triose phosphates, while v_7 is the degradation of extracellular pyruvate/acetaldehyde and J is the net flux of pyruvate/acetaldehyde out of the cell.

The model is based on the following set of rate equations:

$$\frac{dS_1}{dt} = J_0 - v_1 \tag{8a}$$

$$\frac{dS_2}{dt} = 2v_1 - v_2 - v_6 \tag{8b}$$

$$\frac{dS_3}{dt} = v_2 - v_3 \tag{8c}$$

$$\frac{dS_4}{dt} = v_3 - v_4 - J \tag{8d}$$

$$\frac{dN_2}{dt} = v_2 - v_4 - v_6 \tag{8e}$$

$$\frac{dA_3}{dt} = -2v_1 + 2v_3 - v_5 \tag{8f}$$

$$\frac{dS_4^{ex}}{dt} = \varphi J - v_7 \tag{8g}$$

with:

$$v_1 = k_1 S_1 A_3 \left[1 + \left(\frac{A_3}{K_I}\right)^q\right]^{-1} \tag{9a}$$

$$v_2 = k_2 S_2 N_1 \tag{9b}$$

$$v_3 = k_3 S_3 A_2 \tag{9c}$$

$$v_4 = k_4 S_4 N_2 \tag{9d}$$

$$v_5 = k_5 A_3 \tag{9e}$$

$$v_6 = k_6 S_2 N_2 \tag{9f}$$

$$v_7 = k S_4^{ex} \tag{9g}$$

A_2 and A_3, and N_1 and N_2 denote the concentrations of ADP and ATP, and NAD^+ and NADH, respectively. Since several glycolytic reactions are omitted and other reactions are lumped, the model variables denote, in some cases, the concentrations of pools of intermediates, rather than concentrations of individual compounds. This concerns the pool of the triose phosphates, glyceraldehyde 3-phosphate and dihydroxyacetone phosphate (variable S_2), and the pool of pyruvate and acetaldehyde (variable S_4). The concentration of glucose is represented by the variable S_1, and that of 1,3-bisphosphoglycerate by S_3. S_4^{ex} denotes the concentration of the coupling substance in the external solution. Furthermore, the lumping process implies that the concentrations of some compounds do not appear as separate model variables. The differential equations for N_1 and A_2 are omitted, because these concentrations follow from the conservation conditions

$$N_1 + N_2 = N = \text{constant} \tag{10a}$$

$$A_2 + A_3 = A = \text{constant} \tag{10b}$$

φ denotes the ratio of the total cellular volume to the extracellular volume. K_I and q are the inhibition constants and the cooperativity coefficient of the ATP inhibition, respectively. For the transmembrane fluxes, we use

$$J_0 = k_0 G_{ex} \tag{11a}$$

and

$$J = \kappa(S_4 - S_4^{ex}) \tag{11b}$$

In these equations, G_{ex} denotes the concentration of external glucose which is considered to be constant, κ a rate constant which is directly related to the permeability of the membrane. For a more detailed description of this model the reader is referred to the work by Wolf and Heinrich [20].

4. Methods

The model's differential equations (Eqs. (8–9)) were solved numerically by use of the FORTRAN subroutine LSODE [38]. The calculations were performed on a Macintosh computer using Absoft's FORTRAN 77 compiler for the Macintosh, version 4.4 [39]. Calculations involving stochastic fitting (see below) were run on a Unix workstation at Stavanger University College.

In the stochastic fitting method the activation energies E_j of the rate constants k_j (Eq. (2)) and the enthalpy $\Delta H^0_{K_I}$ of K_I were varied randomly until a certain target function $P_{tar}(T)$ was approached closely enough by the numerically calculated period $P(T)$. This was achieved by calculating the root-mean-square deviation χ

$$\chi = \sqrt{\sum_i \left[P_{tar}(T_i) - P(T_i)\right]^2} \tag{12}$$

for a variety of temperature points T_i for an iterative but random choice of activation energies (which are chosen within a certain activation energy interval). During the iteration only those activation energies were kept that led to a decrease in χ. The FORTRAN function RAN1 [40] was used as the random number generator. For a given reference temperature T_{ref} (see below) and activation energy E_j, the pre-exponential factor A_j of process 'j' is calculated by means of the T_{ref} assigned rate constant value k_j by use of the Arrhenius equation, Eq. (2), i.e.

$$A_j = k_j \exp\left(E_j / RT_{ref}\right) \tag{13}$$

5. Results

5.1. Control coefficients

To investigate the conditions for temperature compensation by using Eq. (7), we determined the control coefficients $C_j = \partial \ln f / \partial \ln k_j$ and $C_{K_I} = \partial \ln f / \partial \ln K_I$. First, a reference temperature T_{ref} and a reference state of limit cycle oscillations was chosen with parameters listed in Table 1 (and figure legends) and using for integration initial

Table 1
Parameter values of the reference state[a]

Parameter	Value
J_0	2.5 mM/min
k_1	100.0 mM/min
k_2	6.0 mM/min
k_3	16.0 mM/min
k_4	100.0 mM/min
k_5	1.28/min
k_6	12.0 mM/min
k	1.8/min
κ	13.0/min
q	4.0
K_I	0.52 mM
N	1.0 mM
A	4.0 mM
φ	0.1

[a] Resulting in a period length of 1.17 min. A description of the parameters can be found in Section 3.

concentrations given in Table 2. Then, the periods for varying individually the k_i's (including K_I) are calculated by keeping all other k_j's ($i \neq j$) constant. Fig. 2 shows the relationships $\ln P$ vs. $\ln k_i$ for those rate constants for which the control coefficients C_i varied most with varying k_i. The control coefficients for the reference state are listed in Table 3 (calculations have been performed for 1% variations and for 10% variations of the rate constant and of the inhibition constant K_I. From the ten adjustable parameters only three contribute positively to the period, i.e. when increasing k_i an increase of the period is observed; see Table 3. Among the positive contributions the input flux J_0 has the largest influence. From the parameters with a negative contribution to the period, the rate constant k_5 of nonglycolytic ATP consuming processes exerts the strongest effect.

5.2. Temperature dependency of the oscillations and conditions for temperature compensation

The condition of Eq. (6) or Eq. (7) implies that, theoretically, there should be an infinite number of activation energy combinations leading to temperature compensation. We have tested the applicability of condition given by Eq. (7) using the stochastic fitting method described above to model the experimental period–temperature relationship and temperature-compensated conditions.

First, we determined by a stochastic fit, a set of activation energies which gives a good description of the temperature dependency of the oscillation period to the experimental data of Betz and Chance ([24]; shown as open diamonds in Fig. 3) and Hemker et al. (unpublished; shown as open squares and a thick solid line in Fig. 3). The corresponding activation energies are given in Fig. 5a and in the first column of Table 4. Large solid points in Fig. 3 show the result of a stochastic fit of the model to the data by Hemker et al. While experimental period lengths have been observed as low as 0.2 min, the model stops showing oscillations at approximately 0.8 min. Within the oscillatory range of the model, however, there is a good agreement between experiment and calculations. The considerable dominance of negative contributions in the balancing sum, Eq. (6), is reflected by the fact that the period decreases rapidly with increasing temperature (see $\sum_i C_{k_i} E_i$ in last row of Table 4).

Table 2
Initial concentrations for reference state oscillations

Compound	Concentration (mM)
Glucose	1.187
Glyceraldehyde-3-P/dihydroxyacetone-P	0.193
1,3-Bisphosphoglycerate	0.050
Pyruvate/acetaldehyde	0.115
External pyruvate/acetaldehyde	0.077
ADP	1.525
ATP	2.475
NAD^+	0.923
NADH	0.077

Fig. 3 also shows a set of seven series where the oscillator's ability to show temperature compensation was tested. Corresponding NADH-oscillations are shown in Fig. 4 where part (a) gives three examples for the model fitted to the experimental data whereas parts (b)–(d) show examples for temperature-compensated oscillations of series 1, 3 and 6. When calculating the balancing sums for these sets (last row in Table 4) it is clearly seen that these sums are now close to zero which corresponds to the condition for temperature compensation given in Eq. (6).

With a given set of control coefficients there is clearly a certain variability in the activation energies necessary to satisfy Eq. (6) and thus achieve temperature compensation. Since the balancing sum for the model fitted to the experimental data is negative (Table 4) temperature compensation can either be achieved by decreasing the activation energies of steps with negative control coefficients or by increasing the activation energies of steps with positive control coefficients. This is in accord with the three different activation energy profiles shown in Fig. 5b–d which all result in temperature-compensated oscillators with a period of approximately 2.5 min. It is seen that a common feature of these profiles is the high activation energy E_{J_0} of the input flux which has a positive control coefficient. In fact, increasing E_{J_0} alone

Table 3
Control coefficients C_i for the oscillation period in the reference state

Control coefficient	Value ($\pm 1\%$ variation)	Value ($\pm 10\%$ variation)
C_{J_0}	+0.69	+0.68
C_{k_1}	−0.21	−0.23
C_{k_2}	+0.04	+0.06
C_{k_3}	−0.01	−0.01
C_{k_4}	+0.26	+0.27
C_{k_5}	−1.24	−1.27
C_{k_6}	−0.26	−0.28
C_k	−0.13	−0.12
C_κ	−0.17	−0.15
C_{K_1}	−0.86	−0.84
$\sum_i C_i$ (without K_1)	−1.02	−1.05
$\sum_i C_i$ (with K_1)	−1.88	−1.89

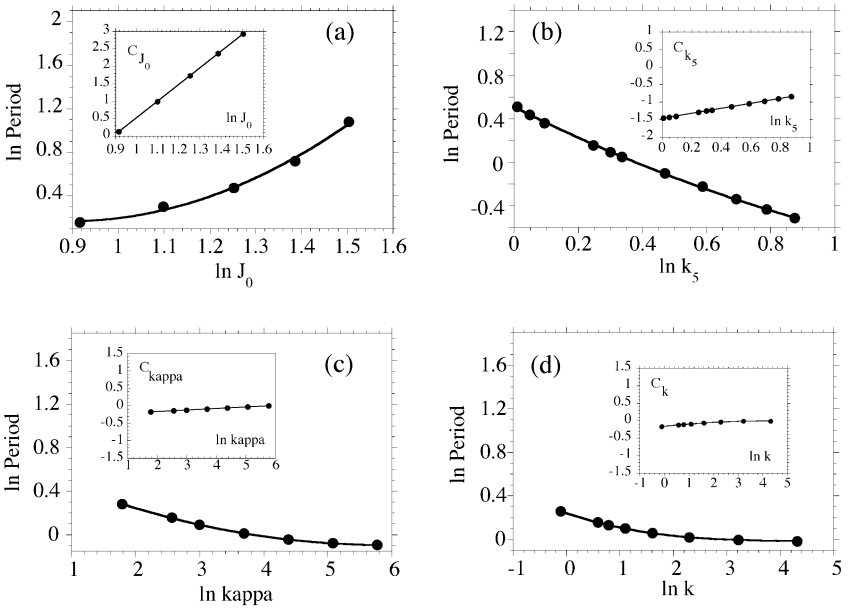

Fig. 2. Determination of the control coefficients C_i by plotting the logarithm of the period against the logarithm of the varying rate constant. The four cases with the greatest variations in C_i as a function of $\ln k_i$ (insets) are shown in figures (a)–(d). Determined C_i values are shown in Table 3.

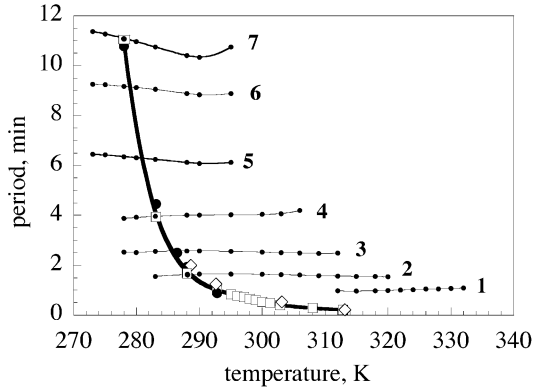

Fig. 3. Horizontal lines (1)–(7): Temperature-compensated oscillations with different periods. Reference parameter values: (1) $T_{ref}=300$ K, $J_0=1.0$ mM/min, $k_1=25$ mM/min, $k_2=2.0$ mM/min, all other parameter values as in Table 1; E_i's are given in Table 4; (2) $T_{ref}=300$ K, $k_1=25$ mM/min, $k_2=2.0$ mM/min, $k_5=2.2$/min, all other parameter values as in Table 1; $E_{J_0}=39.8$ kJ/mol, $E_{k_1}=17.1$ kJ/mol, $E_{k_2}=9.9$ kJ/mol, $E_{k_3}=29.2$ kJ/mol, $E_{k_4}=39.2$ kJ/mol, $E_{k_5}=14.3$ kJ/mol, $E_{k_6}=23.7$ kJ/mol, $E_k=31.3$ kJ/mol, $E_{\text{kappa}}=23.7$ kJ/mol, $E_{K_I}=12.3$ kJ/mol; (3) $T_{ref}=305$ K, $k_1=25$ mM/min, $k_2=2.0$ mM/min, all other parameter values as in Table 1; E_i's are given in Table 4; (4) $T_{ref}=312$ K, $J_0=4.1$ mM/min, $k_1=25$ mM/min, $k_2=2.0$ mM/min, $k_5=1.1$/min, all other parameter values as in Table 1; $E_{J_0}=45.8$ kJ/mol, $E_{k1}=15.2$ kJ/mol, $E_{k_2}=10.5$ kJ/mol, $E_{k_3}=31.1$ kJ/mol, $E_{k_4}=45.4$ kJ/mol, $E_{k_5}=13.3$ kJ/mol, $E_{k_6}=21.2$ kJ/mol, $E_k=32.6$ kJ/mol, $E_{\text{kappa}}=20.0$ kJ/mol, $E_{K_I}=12.3$ kJ/mol; (5) $T_{ref}=312$ K, $J_0=4.3$ mM/min, $k_1=25$ mM/min, $k_2=2.0$ mM/min, $k_5=0.7$/min, all other parameter values as in Table 1; $E_{J_0}=42.0$ kJ/mol, $E_{k_1}=15.3$ kJ/mol, $E_{k_2}=10.7$ kJ/mol, $E_{k_3}=28.4$ kJ/mol, $E_{k_4}=44.1$ kJ/mol, $E_{k_5}=13.3$ kJ/mol, $E_{k_6}=23.0$ kJ/mol, $E_k=29.6$ kJ/mol, $E_{\text{kappa}}=20.2$ kJ/mol, $E_{K_I}=11.7$ kJ/mol; (6) $T_{ref}=318$ K, $J_0=4.5$ mM/min, $k_1=20$ mM/min, $k_2=1.5$ mM/min, $k_4=150$ mM/min, $k_5=0.7$/min, $K_I=0.45$ mM, all other parameter values as in Table 1; E_i's are given in Table 4; (7) $T_{ref}=312$ K, $J_0=4.7$ mM/min, $k_1=20$ mM/min, $k_2=1.5$ mM/min, $k_4=150$ mM/min, $k_5=0.7$/min, $K_I=0.37$ mM, all other parameter values as in Table 1; E_i's are given in Table 4. Open diamonds: experimental data by Betz and Chance [24]. Open squares: experimental data by Hemker et al. (unpublished). Thick solid line: smoothed curve of Hemker et al. data. Large solid dots: fit of model to Hemker et al. data; $T_{ref}=286.5$ K, $k_1=25$ mM/min, $k_2=2.0$ mM/min, all other parameter values as in Table 1; E_i's are given in Table 4.

makes the period of the oscillations less temperature-sensitive as shown in Fig. 6. Moreover, the activation energy of nonglycolytic ATP-consumption (step 5) which is characterized by a strong negative control coefficient is decreased for temperature-compensated oscillations. The same holds true for the enthalpy which enters the temperature dependence of the inhibition constant K_I. The values of the other activation energies for steps with lower absolute values of the control coefficients are more variable.

6. Discussion

6.1. Control coefficients and approximate description of period

The results shown in Fig. 3 and Table 4 show clearly that the model of glycolytic oscillations can be easily temperature-compensated with Eq. (6) as an indicator when temperature compensation is expected to occur. The suitability of Eq. (6) to predict temperature compensation has been shown for several other chemical and biological oscillator models [10,41,42]. On the basis of the performed sensitivity analysis it may be appropriate to approximate the oscillator's period P, Eq. (3), by the expression

$$P \cong h(k_1,\ldots,k_N) = \tau_0 \prod_i \left(\frac{k_i}{k_{i,0}}\right)^{C_i} \qquad (14)$$

which results from a logarithmic expansion of the function $P(k_1,\ldots, k_N)$ around a reference state characterized by the rate constants $k_{i,0}$ and the reference period τ_0 [10,41]. According to the summation theorem for control coefficients of oscillatory periods the following relation is fulfilled

$$\sum_i C_i = -1 \qquad (15)$$

[25,28,43]. Eq. (15) reflects the fact that the period is a homogeneous function of the rate constants of degree -1. For larger deviations of the rate constants from their reference values Eq. (14) is only approximately fulfilled. Some (temperature-sensitive) parameters (for example K_I) may not enter the rate equations in a homogenous form as most of the rate constants normally do. In this case, the period will still depend on that parameter (as is

Table 4
Testing the balancing equation, Eq. (6)

Parameter	E_i, kJ/mol (experimental)[a]	E_i, kJ/mol (series 1)	E_i, kJ/mol (series 3)	E_i, kJ/mol (series 6)	E_i, kJ/mol (series 7)
J_0	16.2	43.9	46.1	41.4	51.0
k_3	44.9	31.7	48.7	30.4	39.2
k_4	58.7	44.2	38.0	48.1	42.4
k_1	13.8	16.0	19.1	14.0	23.3
k_2	60.7	10.4	11.8	10.8	11.9
k_5	41.2	13.3	17.9	15.1	19.8
k_6	31.4	23.7	16.2	24.0	15.7
κ (kappa)	15.9	22.3	19.0	18.7	19.7
k	24.3	30.0	32.2	34.1	31.5
K_I[b]	47.0	12.2	11.4	8.6	10.0
$\sum_i C_{k_i} E_i$	−79.0	−2.3	−6.1	−1.8	−3.6

For calculating the balance sums $\sum_i C_{k_i} E_i$ (last row), values for control coefficients have been used corresponding to a 10% change of parameters (cf. Table 3).

[a] Fit to Hemker et al. data, Fig. 3 (large solid dots).

[b] In case of K_I, E_i is interpreted as $\Delta H^0_{K_I}$.

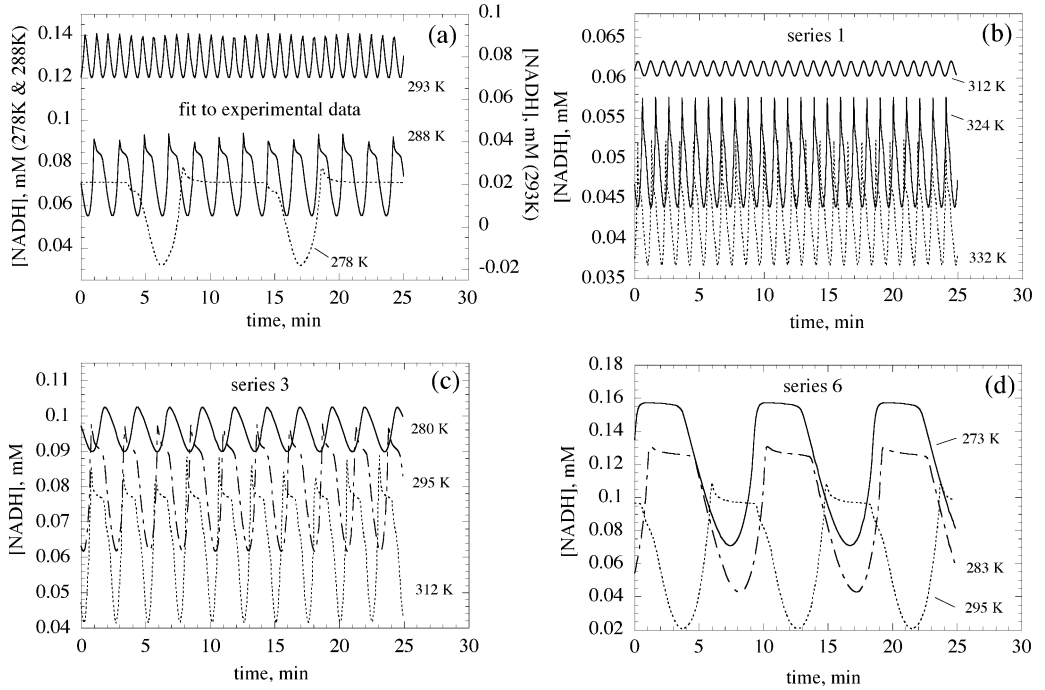

Fig. 4. Amplitudes and form of oscillations. (a) Fit to Hemker et al. data (Fig. 3). With increasing temperature the amplitude decreases as found experimentally (Chance et al. [45]). (b) and (c) The amplitude for the temperature-compensated oscillations increases with increasing temperature, but this effect becomes less important for larger period lengths.

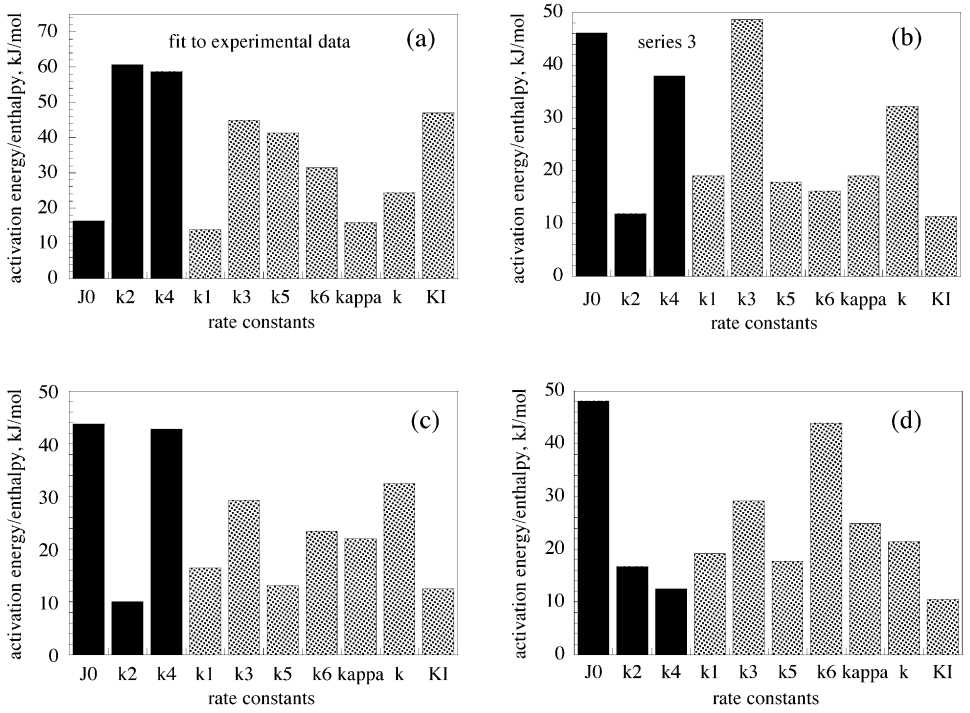

Fig. 5. (a) Activation energy profile for the fit to experimental value as shown in Fig. 3. Note the small contribution of the influx parameter J_0 to the period's temperature sensitivity. (b)–(d) Different activation energy profiles for temperature-compensated sets with periods close to 2.5 min. In (c) we have the same reference parameter values as in (b), but $T_{ref} = 300$ K instead of 305 K. In (d) we have the same reference parameter values as in (b), but $T_{ref} = 290$ K instead of 305 K. Note the large contribution of the influx parameter J_0 to the period's temperature insensitivity.

the case for K_I) but the summation theorem Eq. (15) will not be applicable (see Table 3 where the control coefficients of K_I have been considered separately from the control coefficients of the rate constants).

6.2. Temperature range for temperature compensation

Because the control coefficients C_i (Table 3) must be regarded as local quantities characterizing the effects of small perturbations, predictions for temperature compensation by Eq. (6) may not be optimal over the whole temperature range. For example, by increasing only E_{J_0} as shown in Fig. 6 temperature compensation can be obtained for a relatively small temperature range. However, to improve temperature compensation over a larger temperature range a 'fine-tuning' of all activation energies is necessary. This can be either done manually or by the stochastic fit method as described above. Even then, temperature compensation is only observed in a certain and finite temperature range and generally not over the whole parameter range where oscillations can be observed. Although this appears at first as an insufficiency in a model's performance, such local temperature compensation is generally observed in biological clock oscillators. For example, in the circadian clock rhythm of *Neurospora crassa*, temperature compensation is only observed in the temperature range $\approx$15–30 °C. Above this range *Neurospora's* circadian period decreases more rapidly similar to what is normally observed experimentally in chemical (or biochemical) oscillators [44].

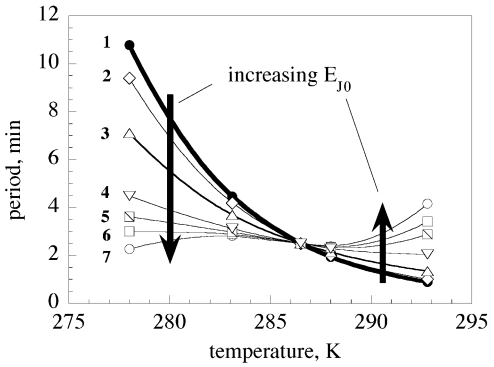

Fig. 6. Increase of E_{J_0} makes the period less temperature-sensitive. (1) Thick solid line, same system as thick solid line in Fig. 3, with $E_{J_0}=16.2$ kJ/mol, $\sum_i C_i E_i = \Sigma = -78.1$ (see also Table 4); (2) $E_{J_0}=32$ kJ/mol, $\Sigma=-68.3$; (3) $E_{J_0}=64$ kJ/mol, $\Sigma=-46.5$; (4) $E_{J_0}=100$ kJ/mol, $\Sigma=-22.0$; (5) $E_{J_0}=110$ kJ/mol, $\Sigma=-15.2$; (6) $E_{J_0}=115$ kJ/mol, $\Sigma=-11.8$; (7) $E_{J_0}=120$ kJ/mol, $\Sigma=-8.4$.

6.3. Amplitude behavior

The amplitudes of the model's oscillations fitted to the experimental period–temperature relationship (Fig. 3a) have been found to decrease with increasing temperature (Fig. 4a) in agreement with experimental results [45]. On the other hand, when inspecting the amplitudes of the temperature-compensated oscillations (Fig. 4b–d) one sees the opposite trend, i.e. with increasing temperature the amplitudes of the oscillations increase. This effect becomes less pronounced as the period of the temperature-compensated oscillations is forced to larger values. An increase in amplitude with increasing temperature has been observed in other temperature-compensated models as well [10]. The behavior can be explained by phase-space arguments as the velocity of the trajectory in phase space increases with increasing temperature, the oscillator must travel through a larger area in phase space to keep the same period. Thus, the amplitude in temperature-compensated systems is expected to increase with increasing temperature. In their 'amplitude model', Lakin-Thomas et al. [46] have studied the consequences of this behavior for the resetting of the circadian clock in *Neurospora crassa*. It may be noted, however, that Leloup and Goldbeter [47] found in a model for the circadian rhythm of *Drosophila* a situation with apparently contrary behavior, i.e. a birhythmic state where the low amplitude oscillations have a larger period than the high amplitude oscillations. In the case of birhythmicity, two stable limit cycles of distinct period length and amplitude can occur for the same set of rate constants and other parameter values. Although the observations by Leloup and Goldbeter might at first sight be considered as a counter-example concerning the generality of the amplitude model, it has to be tested how the amplitudes for each of the two coexisting limit cycles behave in a temperature-compensated case. As described in this study and in Ref. [10], it still could be (and in agreement with the amplitude model) that in the temperature-compensated case the amplitude for at least one of the coexisting limit cycles increase with increasing temperature.

6.4. Glucose transport kinetics

As shown in Fig. 2a and Table 3 glucose influx J_0 across the plasma membrane has a high influence on the period length in the model. When allowing a free float of all activation energies and fitting period lengths to those experimentally observed for various temperatures (Fig. 3), an activation energy for E_{J_0} of approximately 16 kJ/mol is obtained (Table 4), which is a little lower than the activation energy that can be calculated for free diffusion of glucose in water (see for example Ref. [48]). Experimentally, the kinetics of two glucose transport systems have been studied in vesicles of *Saccharomyces cerevisiae*, one showing Michaelis–Menten type kinetics (facilitated diffusion transport) while the other shows first-order behavior (entry through a pore). In both cases, the experimentally determined activation energies lie in the range of 60 and 30 kJ/mol, respectively [49]. This means, our calculated value for E_{J_0} differs from the experimental value by a factor of 0.25–0.5.

Reijenga et al. [50] studied the effect of hexose transport on the dynamics of glycolytic oscillations in *Saccharomyces cerevisiae* cells. They found that transport of hexoses into the cells have a marked influence on the oscillations. By partial blocking

the influx of glucose into the cells using maltose the authors found an increase in frequency with an increase of the glucose influx. The Reijenga et al. in vivo studies are also in agreement with earlier experiments performed on cell extracts [51], where it was found that the frequency of the oscillations increased with increasing input rate of substrate glucose or fructose. Although the model studied here shows a considerable influence of the glucose influx on the period, the experimental findings by Reijenga et al. [50] are opposite to the J_0-influence in the model, which predicts a *decrease* in frequency with an increase of glucose influx J_0 (Fig. 2a). The reason for this discrepancy is not clear, but it could be related to the complex regulation of glucose uptake by different hexose transporters [52,53] or to the type of PFK regulation considered in the studied model. Although models based on activation of PFK [32] or pyruvate kinase [54] are in agreement with the experimental relationship between frequency and glucose influx, a check of frequency control coefficients [29,55,56] showed that even more detailed models such as the 'full-scale model' of Hynne et al. [33] do not reflect the experimentally observed negative effect of the glucose influx on the oscillatory period.

6.5. Experimental temperature-compensated yeast glycolytic oscillators?

An interesting question is whether it would be possible to obtain yeast mutants which have a glycolytic oscillator that is less temperature sensitive or even temperature-compensated. As indicated by this study and also by experiments [50], the influx of glucose into the cells seems to play an important role in the control of glycolytic dynamics. Therefore, a possible start in the search for a temperature-compensated-glycolytic oscillator may be to look at the oscillator's temperature behavior in hexose transport mutants [53].

However, using glycolytic oscillator models as guidelines is somewhat problematic. Mainly because the different models have different sensitivities against parameter changes and also focus on different aspects of the oscillations [29,56]. An extensive comparison between in vivo behavior of yeast glycolysis and the in vitro kinetic properties of the constituent enzymes showed considerable discrepancies and for only 50% of the enzymes the in vitro kinetics did describe the in vivo activity satisfactorily [57]. Although the dynamics of the glycolytic oscillations in yeast are still not completely understood, model calculations in combination with site directed mutation experiments on the hexose transporter genes [53] could still be useful in order to make yeast mutants which have a less temperature-sensitive-glycolytic oscillator.

7. Conclusion

We have shown that temperature compensation is possible in a detailed model [20] for glycolytic oscillations. Using the same strategy, conditions for temperature compensation in other glycolytic oscillator models should be obtainable. By affecting the kinetics and activation energies for one or several component processes with molecular biology methods it might even be possible to construct yeast mutants which show temperature-compensated glycolytic oscillations. Such mutants may not only be of importance for an understanding of the molecular processes in glycolytic oscillations, but also for our understanding of temperature compensation in biological clocks.

Acknowledgments

We thank Hans Westerhoff for allowing us to use the work by Hemker et al. and for bringing up the idea of a temperature-compensated glycolytic oscillator. We also thank Stefan Müller for helpful correspondence and comments. P.R. thanks Jay Dunlap, Department of Genetics, Dartmouth Medical School for hospitality and support while a final version of the manuscript was prepared.

References

[1] E. Bünning, The Physiological Clock, Springer, Berlin, 1963.
[2] L.N. Edmunds, Cellular and Molecular Bases of Biological Clocks, Springer, New York, 1988.
[3] L. Rensing, U. Meyer-Grahle, P. Ruoff, Biological timing and the clock metaphor: oscillatory and hourglass mechanisms, Chronobiol. Int. 18 (2001) 329–369.

[4] J.C. Dunlap, J.J. Loros, P.J. DeCoursey, Biological Timekeeping, Sinauer Associates, Inc. Publishers, Sunderland, 2003.
[5] Special issue on Temperature compensation: molecular mechanisms and models, Chronobiol. Int. 14 (1997) 445–536.
[6] C.S. Pittendrigh, Temporal organization: reflections of a Darwinian clock-watcher, Ann. Rev. Physiol. 55 (1993) 16–54.
[7] M. Dixon, E.C. Webb, C.J.R. Thorne, K.F. Tipton, Enzymes, Longman, London, 1979.
[8] J.W. Hastings, B.M. Sweeney, On the mechanism of temperature independence in a biological clock, Proc. Natl. Acad. Sci. USA 43 (1957) 804–811.
[9] P. Ruoff, M. Vinsjevik, L. Rensing, Temperature compensation in biological oscillators: a challenge for joint experimental and theoretical analysis, Comments Theor. Biol. 5 (2000) 361–382.
[10] P. Ruoff, Introducing temperature-compensation in any reaction kinetic oscillator model, J. Interdiscipl. Cycle Res. 23 (1992) 92–99.
[11] P. Ruoff, L. Rensing, R. Kommedal, S. Mohsenzadeh, Modeling temperature compensation in chemical and biological oscillators, Chronobiol. Int. 14 (1997) 499–510.
[12] A. Skrabal, Vorlesungsversuch zur Demonstration eines Falles der Abnahme der Reaktionsgeschwindigkeit mit der Temperatur, Z. Elektrochem. 21 (1915) 461–463.
[13] G. Rábai, I. Hanazaki, Temperature compensation in the oscillatory hydrogen peroxide–thiosulfate–sulfite flow system, Chem. Comm. 19 (1999) 1965–1966.
[14] K.M. Kóvacs, G. Rábai, Temperature-compensation in pH-oscillators, Phys. Chem. Chem. Phys. 4 (2002) 5265–5269.
[15] B. Chance, E.K. Pye, A.K. Ghosh, B. Hess, Biological and Biochemical Oscillators, Academic Press, New York, 1973.
[16] S. Danø, P.G. Sørensen, F. Hynne, Sustained oscillations in living cells, Nature 402 (1999) 320–322.
[17] B. Hess, A. Boiteux, Oscillatory phenomena in biochemistry, Ann. Rev. Biochem. 40 (1971) 237–258.
[18] B. Hess, Periodic patterns in biochemical reactions, Q. Rev. Biophys. 30 (1997) 121–176.
[19] P. Richard, B. Teusink, M.B. Hemker, K. Van Dam, H.V. Westerhoff, Sustained oscillations in free-energy state and hexose phosphates in yeast, Yeast 12 (1996) 731–740.
[20] J. Wolf, R. Heinrich, Effect of cellular interaction on glycolytic oscillations in yeast: a theoretical investigation, Biochem. J. 345 (Pt 2) (2000) 321–334.
[21] J.C. Leloup, A. Goldbeter, Temperature compensation of circadian rhythms: control of the period in a model for circadian oscillations of the per protein in *Drosophila*, Chronobiol. Int. 14 (1997) 511–520.
[22] C.I. Hong, J.J. Tyson, A proposal for temperature compensation of the circadian rhythm in *Drosophila* based on dimerization of the PER protein, Chronobiol. Int. 14 (1997) 521–529.
[23] K.R. Valeur, R. degli Agosti, Simulations of temperature sensitivity of the peroxidase–oxidase oscillator, Biophys. Chem. 99 (2002) 259–270.
[24] A. Betz, B. Chance, Influence of inhibitors and temperature on the oscillation of reduced pyridine nucleotides in yeast cells, Arch. Biochem. Biophys. 109 (1965) 579–584.
[25] R. Heinrich, S. Schuster, The Regulation of Cellular Systems, Chapman and Hall, New York, 1996.
[26] R.M. Noyes, Kinetics of complex reactions, Techniques of Chemistry 6, Invest. Rates Mech. React., third ed., (Pt 1) (1974) 489–538.
[27] K.J. Laidler, J.H. Meiser, Physical Chemistry, second ed., Houghton Mifflin Company, Geneva (Illinois), 1995.
[28] H. Kacser, J.A. Burns, The control of flux, Symp. Soc. Exp. Biol. 27 (1973) 65–104.
[29] K.A. Reijenga, H.V. Westerhoff, B.N. Kholodenko, J.L. Snoep, Control analysis for autonomously oscillating biochemical networks, Biophys. J. 82 (2002) 99–108.
[30] U.F. Franck, Feedback kinetics in physicochemical oscillators, Ber. Bunsenges. Phys. Chem. 84 (1980) 334–341.
[31] A. Goldbeter, Biochemical Oscillations and Cellular Rhythms: The Molecular Bases of Periodic and Chaotic Behavior, Cambridge University Press, Cambridge, UK, 1996.
[32] A. Goldbeter, R. Lefever, Dissipative structures for an allosteric model. Application to glycolytic oscillations, Biophys. J. 12 (1972) 1302–1315.
[33] F. Hynne, S. Danø, P.G. Sørensen, Full-scale model of glycolysis in *Saccharomyces cerevisiae*, Biophys. Chem. 94 (2001) 121–163.
[34] O. Richter, A. Betz, C. Giersch, The response of oscillating glycolysis to perturbations in the NADH/NAD system: a comparison between experiments and a computer model, Biosystems 7 (1975) 137–146.
[35] E.E. Sel'kov, Self-oscillations in glycolysis. 1. A simple kinetic model, Eur. J. Biochem. 4 (1968) 79–86.
[36] P. Smolen, A model for glycolytic oscillations based on skeletal muscle phosphofructokinase kinetics, J. Theor. Biol. 174 (1995) 137–148.
[37] Y. Termonia, J. Ross, Oscillations and control features in glycolysis: numerical analysis of a comprehensive model, Proc. Natl. Acad. Sci. USA 78 (1981) 2952–2956.
[38] K. Radhakrishnan, A.C. Hindmarsh, Description and Use of LSODE, the Livermore Solver for Ordinary Differential Equations, National Aeronautics and Space Administration, Lewis Research Center, Cleveland, OH 44135-3191, 1993.
[39] FORTRAN 77 compiler for Macintosh, Absoft Corp., Rochester Hills, MI 48309, USA, 1997.
[40] W.H. Press, B.P. Flannery, S.A. Teukolsky, W.T. Vetterling, Numerical Recipes. The Art of Scientific Comput-

ing (FORTRAN Version), Cambridge University Press, Cambridge, UK, 1989.
[41] P. Ruoff, Antagonistic balance in the Oregonator: about the possibility of temperature-compensation in the Belousov–Zhabotinsky reaction, Physica D 84 (1995) 204–211.
[42] P. Ruoff, L. Rensing, The temperature-compensated Goodwin model simulates many circadian clock properties, J. Theor. Biol. 179 (1996) 275–285.
[43] P.F. Baconnier, P. Pachot, J. Demongeot, An attempt to generalize the control coefficient concept, J. Biol. Syst. 1 (1993) 335–347.
[44] G.F. Gardner, J.F. Feldman, Temperature compensation of circadian periodicity in clock mutants of *Neurospora crassa*, Plant Physiol. 68 (1981) 1244–1248.
[45] B. Chance, R.W. Estabrook, A. Ghosh, Damped sinusoidal oscillations of cytoplasmic reduced pyridine nucleotide in yeast cells, Proc. Natl. Acad. Sci. USA 51 (1964) 1244–1251.
[46] P.L. Lakin-Thomas, S. Brody, G.G. Cote, Amplitude model for the effects of mutations and temperature on period and phase resetting of the *Neurospora* circadian oscillator, J. Biol. Rhythms 6 (1991) 281–297.
[47] J.C. Leloup, A. Goldbeter, Chaos and birhythmicity in a model for circadian oscillations of the PER and TIM proteins in *Drosophila*, J. Theor. Biol. 198 (1999) 445–459.
[48] W.D. Stein, Transport and Diffusion Across Cell Membranes, Academic Press, San Diego, 1986.
[49] C. Reinhardt, B. Volker, H.J. Martin, J. Kneiseler, G.F. Fuhrmann, Different activation energies in glucose uptake in *Saccharomyces cerevisiae* DFY1 suggest two transport systems, Biochim. Biophys. Acta 1325 (1997) 126–134.
[50] K.A. Reijenga, J.L. Snoep, J.A. Diderich, H.W. van Verseveld, H.V. Westerhoff, B. Teusink, Control of glycolytic dynamics by hexose transport in *Saccharomyces cerevisiae*, Biophys. J. 80 (2001) 626–634.
[51] B. Hess, A. Boiteux, Biological and biochemical oscillators, in: B. Chance, E.K. Pye, A.K. Ghosh, B. Hess (Eds.), Substrate Control of Glycolytic Oscillations, Academic Press, New York, 1973, pp. 229–241.
[52] A.L. Kruckeberg, The hexose transporter family of *Saccharomyces cerevisiae*, Arch. Microbiol. 166 (1996) 283–292.
[53] S. Özcan, M. Johnston, Function and regulation of yeast hexose transporters, Microbiol. Mol. Biol. Rev. 63 (1999) 554–569.
[54] V.V. Dynnik, E.E. Sel'kov, On the possibility of self-oscillations in the lower part of the glycolytic system, FEBS Lett. 37 (1973) 342–346.
[55] M. Bier, B.M. Bakker, H.V. Westerhoff, How yeast cells synchronize their glycolytic oscillations: a perturbation analytic treatment, Biophys. J. 78 (2000) 1087–1093.
[56] B. Teusink, B.M. Bakker, H.V. Westerhoff, Control of frequency and amplitudes is shared by all enzymes in three models for yeast glycolytic oscillations, Biochim. Biophys. Acta 1275 (1996) 204–212.
[57] B. Teusink, J. Passarge, C.A. Reijenga, et al., Can yeast glycolysis be understood in terms of in vitro kinetics of the constituent enzymes? Testing biochemistry, Eur. J. Biochem. 267 (2000) 5313–5329.